Effects of transmetalation on the mechanisms of copper-catalyzed phenolic oxidative coupling reactions

Atieh Abu-Raqabah*, Geoffrey Davies**
Department of Chemistry, Northeastern University, Boston, MA 02115 (USA)
and Mohamed A. El-Sayed**
Department of Chemistry, Faculty of Science, Alexandria University, Alexandria (Egypt)

(Received July 24, 1991)

Abstract

The mechanism of initiation of phenolic oxidative coupling by the tetranuclear copper(I) complex $[pyCuCl]_4$ is affected by transmetalation. $[pyCuCl]_4$ is stoichiometrically transmetalated by equimolar $(M(NS)_2$ reagents (M is Co, Ni, Cu or Zn) at room temperature in nitrobenzene under N_2 to give equimolar solutions of air-sensitive complexes $py_3Cu_3M(NS)Cl_4$ (**IIa–d**, respectively) and py and 1 mol of insoluble Cu(NS)(s). The corresponding reaction with equimolar $Co(NS)_3$ gives equimolar solutions of $py_3Cu_3Co(NS)_2Cl_4$ (**III**) and py and 1 mol of Cu(NS)(s). Here, py is pyridine and NS is monoanionic *S*-methyl isopropylidenehydrazinecarbodithioate. Second-order reduction of O_2 by $[pyCuCl]_4$ gives the tetranuclear oxocopper(II) complex $(\mu_4\text{-}O)py_4Cu_4Cl_4O$ (**Ib**). Reduction of O_2 by **IIc** in the presence of equimolar py gives **Ib** and the disulfide co-product N_2S_2. The corresponding reductions of O_2 by **IIa**, **IIb**, **IId** and **III** give products $py_3CuMCl_4O_2$ (**IVa**, **IVb**, **IVd** and **IVa**, respectively) and N_2S_2. Insertion of O_2 through the Cl_4 cores of the reductants is the rate-determining step in each system. However, different product core structures are indicated by different spectral sensitivity to oxidation co-product N_2S_2 and by different rate laws for their oxidation of 2,6-dimethylphenol (DMPOH) to the corresponding diphenoquinone. These core structures apparently contain either a weakly basic Cu–O–M unit (in **IVa** and **IVb**) or a strongly basic Cu_v–O unit (in **Ib** and **IVd**). As a result, the rates of oxidation of DMPOH by **Ib** and **IVd** are independent of [DMPOH]. Opening of the Cu–O–M unit to give a weakly basic site M_v–O is proposed to explain induction periods in the **IVa**, **IVb**/DMPOH systems, which then proceed at rates which are proportional to [DMPOH]. The origin of different $py_{3,4}Cu_3MCl_4O_2$ product core structures is discussed.

Introduction

Equation (1) is an example of oxidative coupling reactions that are initiated by halo(amine)copper(I) complexes [1, 2]. Reactions (1) are attractive because: (i) coupling processes that are catalyzed under mild conditions by common elements like copper are inherently useful and economical; (ii) phenol reductants engage prominently in natural systems and especially in those involving copper(I)/copper(II)/O_2 reactions [3, 4]; (iii) reactions (1a) are polymerizations of the third kind, the others being free-radical and condensation polymerizations [1, 5, 6]; (iv) the polyphenylene oxide products of eqn. (1a) have excellent thermal, mechanical and insulating properties that can be varied by choice of R and by blending with other polymers [1, 6]; (v) quinones are important biological materials that participate in a wide variety of redox processes [7].

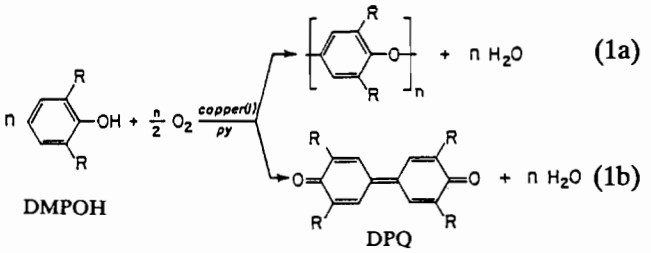

Much less is known about the mechanisms of metal-catalyzed oxidative coupling reactions than about other polymerization processes [2, 8–10]. Because of the commercial value of the polymeric products [1, 5, 6], detailed studies have been made of the effects of R, copper ligands and other experimental parameters that favor reaction (1a) over (1b) [1]. Bidentate *N*-alkyldiamines L are among the best copper ligands for catalysis of reactions (1) [1]. A recent study with L = *N*,*N*,*N*′,*N*′-tetraethylethylenediamine (TEED) indicates that oxocopper(II) dimer $L_2Cu_2Cl_2O$ is the likely catalyst for reaction (1a) at temperatures above −25 °C [11].

*Current address: SABIC R&D, P.O. Box 42503, Riadh 11551, Saudi Arabia.
**Authors to whom correspondence should be addressed.

0020-1693/92/$5.00

The cheapest effective copper ligand for catalytic reactions (1) is pyridine (py) [1]. Studies have shown that py/CuX/phenol reactant ratios and temperature affect the product distributions but that reaction (1b) always occurs to some extent [1, 9]. The use of substituted pyridines gives less active catalytic systems than are obtained with py [1, 2, 8].

Oxidation of slurries of CuCl and CuBr with O_2 in methylene chloride at molar ratio [py]/[CuX] = 0.75 gives solutions of brown, EPR-inactive oxocopper (II) complex $py_3Cu_4X_4O_2$ (**Ia**) that react with 1 mol of py to give EPR-active $py_4Cu_4X_4O_2$ (**Ib**) [12]. The latter also has a very high affinity for py [13] and ultimately gives py_2CuX_2 and polymeric $(py_mCuO)_n$, exactly as observed on oxidation of slurries of CuCl and CuBr in neat py [14].

All the oxo(pyridine)copper(II) complexes cited are initiators for reaction (1) but the change of product distribution with experimental conditions [1] is difficult to understand because monomeric, dimeric and tetrameric copper(I) species exist at different [py] [8, 12] and the oxocopper(II) products are very sensitive to added py [13].

Despite the experimental handicaps, it has been concluded that there are two major components in catalytic reactions (1). One involves deprotonation of the phenol by oxocopper(II) and oxidation of coordinated phenolate by copper(II). The other, which completes the cycle, is rapid reoxidation of copper(I) to copper(II) by O_2 (Scheme 1) [2, 15]. Getting at the molecular details of these components is difficult because most efficient oxocopper(II) initiators are inherently unstable resting species [8, 13–15]. This is especially true of $py_{3,4}Cu_4X_4O_2$ complexes, which disproportionate to inactive species on attempted isolation [8, 13–15]. Nevertheless, we know that **Ia** and **Ib** are tetranuclear, four-electron oxidants, which matches the redox requirements of reactions (1) [15]. By comparison with properties of isolatable but inactive dioxocopper(II) complexes, it was proposed that **Ia** and **Ib** have the following core structures [8, 12, 13]. These structures have distinguishable copper sites v and x; the v site apparently carries a terminal (and, therefore, strongly basic) [16] oxo group [8, 12].

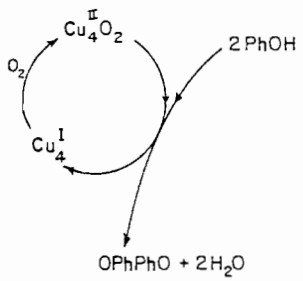

Scheme 1.

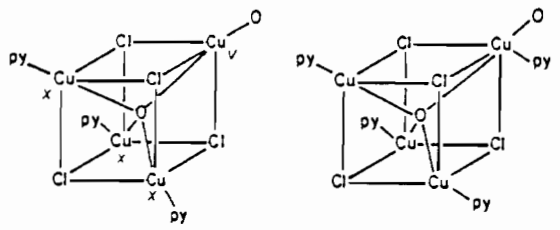

Ia **Ib**

How can we verify that the v site [12, 15] is responsible for initiator and catalytic activity in eqn. (1) given the limited extent to which the system can be manipulated without undergoing drastic molecular change? We cannot substitute the amine ligands in pyridinecopper(I) or oxo(pyridine)copper(II) complexes without risking the formation of different structures [8, 13–15]. But we can directly substitute other metals for copper by transmetalation with reagents **A** and **B** [17–23]. Substitution of redox-inactive metals reduces the oxidative capacity of **Ia, b** and could affect the rates and product distribution of reactions (1).

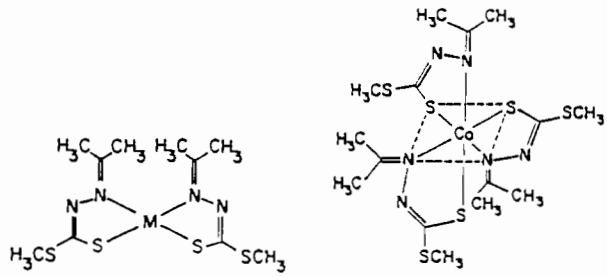

A **B**

Replacement of all the copper(II) in **Ia** by transmetalation with $x = 4$ mol of $Ni(NS)_2$ (NS is monoanionic S=methyl isopropylidinehydrazinecarbodithioate in **A** and **B**) in eqn. (2) destroys its initiator and catalytic activity [17].

$$\mathbf{Ia} + x\mathrm{Ni(NS)_2} \longrightarrow (\mu_4\text{-O})\mathrm{py_3Cu_{4-x}Ni_xCl_40 \cdot Cu(NS)_2} + (x-1)\mathrm{Cu(NS)_2} \qquad (2)$$

This is a clear indication that catalytic mechanisms can be altered by transmetalation. Unfortunately, the partially transmetalated products of reactions (2) are too unstable to be isolated as solids [17, 24]: examination of the reactions of partially transmetalated products with phenols is also complicated by the presence of co-product $Cu(NS)_2$, which has mild catalytic activity and associates strongly with $(\mu_4\text{-O})py_3Cu_{4-x}Ni_xCl_4O$ (eqn. (2)). We have found that attempted removal of $Cu(NS)_2$ destroys the initiator species of interest [24].

Here we describe an alternative transmetalation approach based on replacement of one copper(I) center in $[pyCuCl]_4$ [15] with another metal M = Co, Ni, Cu or Zn from reagents **A** and **B** through reactions (3) and (4). We find that $py_3Cu_3M(NS)Cl_4$ (M = Co, Ni,

Zn) and **III** are oxidized by O_2 to $py_3Cu_3MCl_4O_2$, eqns. (5) and (6), while equimolar $py_3Cu_3Cu(NS)Cl_4$ and py react with O_2 to give **Ib**, eqn. (7). Reactions (5)–(7) proceed by rate-determining O_2 insertion through the Cl_4 cores of the reductants [8, 18, 19]. However, different spectral sensitivity of $py_{3,\ 4}Cu_3MCl_4O_2$ to co-product N_2S_2 and different rates and rate laws for oxidation of 2,6-dimethylphenol (DMPOH) by $py_{3,\ 4}Cu_3MCl_4O_2$ indicate that they have core structures with differently disposed oxo groups. The origin of these different core structures is discussed.

$$[pyCuCl]_4 + \mathbf{A} \longrightarrow$$

$$py_3Cu_3M(NS)Cl_4 + py + Cu(NS)(s) \quad (3)$$
$$\mathbf{II}$$

$$[pyCuCl]_4 + \mathbf{B} \longrightarrow$$

$$py_3Cu_3Co(NS)_2Cl_4 + py + Cu(NS)(s) \quad (4)$$
$$\mathbf{III}$$

$$py_3Cu_3M(NS)Cl_4 + O_2 \longrightarrow$$

$$py_3Cu_3MCl_4O_2 + 1/2N_2S_2 \quad (5)$$
$$\mathbf{IV}$$

$$py_3Cu_3Co(NS)_2Cl_4 + O_2 \longrightarrow$$

$$py_3Cu_3CoCl_4O_2 + N_2S_2 \quad (6)$$
$$\mathbf{IVa}$$

$$py_3Cu_3Cu(NS)Cl_4 + py + O_2 \longrightarrow$$

$$(\mu_4\text{-}O)py_4Cu_4Cl_4O + 1/2N_2S_2 \quad (7)$$
$$\mathbf{IVc = Ib}$$

Experimental

Materials

Solvent nitrobenzene (Aldrich) was distilled under vacuum from P_2O_5 and stored over 4 Å molecular sieves. Pyridine (Aldrich) was dried over KOH for 24 h, distilled from BaO and stored in the dark over 4 Å molecular sieves. Copper(I) chloride was prepared by the literature method [25]. Transmetalators $M(NS)_2$ (A:M = Co, Ni, Cu, Zn) and $Co(NS)_3$ (**B**) were prepared by published procedures [26]. 2,6-Dimethylphenol (DMPOH: Aldrich) was recrystallized from ethanol/pentane. High purity N_2 was deoxygenated by passage through a freshly activated column of Alfa DE-OX catalyst. Solutions of $[pyCuCl]_4$, **Ia** and **Ib** in nitrobenzene were obtained as described [8, 12, 15].

Synthesis of tetranuclear complexes $py_3Cu_3M(NS)Cl_4$ (M = Co (IIa), Ni (IIb), Cu (IIc), Zn (IId)) and $py_3Cu_3Co(NS)_2Cl_4$ (III)

A deoxygenated solution of the respective transmetalator **A** (1 mmol) in nitrobenzene (20 ml) was added dropwise over a period of 1 h to a clear solution of $[pyCuCl]_4$ [15] (1 mmol) in nitrobenzene (30 ml) under N_2 at room temperature. Each mixture was then stirred under N_2 for 6 h to ensure complete reaction (3). The product mixture was filtered under N_2 to remove precipitated co-product Cu(NS)(s), which was washed with small portions of methylene chloride, dried at 100 °C and weighed to confirm the stoichiometry of eqn. (3) [18]. Attempts to isolate extremely air-sensitive solid products $py_3Cu_3M(NS)Cl_4$ were unsuccessful. However, cryoscopic measurements on the nitrobenzene filtrates from eqn. (3) indicated the presence of equimolar py and $py_3Cu_3M(NS)Cl_4$ (Table 1). Nitrobenzene solutions of equimolar complex $py_3Cu_3Co(NS)_2Cl_4$ (**III**) and py were made from eqn. (4) and identified in the same manner.

TABLE 1. Cryoscopic and electronic spectral data for $[pyCuCl]_4$, the products of transmetalation reactions (3) and (4) and the products of oxidation reactions (5)–(8)

Reaction	Symbol	Complex	M_r[a]	λ_{max} (nm) (ϵ_λ (M^{-1} cm^{-1}))[b]
		$[pyCuCl]_4$[c]	740 ± 20 (712)	d
7, 8[c]	**Ib**	$[pyCuCl]_4O_2$	760 ± 20 (744)	850(810), 775(780)
3	**IIa**	$py_3Cu_3Co(NS)Cl_4$	760 ± 20 (790)	650(445), 630(570) 610(680), 575(520)
3	**IIb**	$py_3Cu_3Ni(NS)Cl_4$	735 ± 20 (790)	d
3	**IIc**	$py_3Cu_3Cu(NS)Cl_4$	770 ± 20 (795)	850(200), 775(200)
3	**IId**	$py_3Cu_3Zn(NS)Cl_4$	820 ± 20 (796)	d
4	**III**	$py_3Cu_3Co(NS)_2Cl_4$	980 ± 20 (950)	850(185), 775(225) 650(670), 630(875) 610(970), 575(825)
5, 6	**IVa**	$py_3Cu_3CoCl_4O_2$	690 ± 20 (661)	850(435), 775(455) 650(720), 630(860) 610(945), 575(810)
5	**IVb**	$py_3Cu_3NiCl_4O_2$	620 ± 20 (660)	850(580), 775(590)
5	**IVd**	$py_3Cu_3ZnCl_4O_2$	620 ± 20 (667)	850(510), 775(540)[e]

[a]Measured in nitrobenzene at the $3–5 \times 10^{-2}$ m level. Data obtained by allowing for the presence of py and N_2S_2 as indicated in eqns. (3)–(7) [18]. [b]In nitrobenzene at 25 °C. [c]See text and ref. 15. [d]No spectral features in the 700–900 nm region. [e]See text for discussion of these data.

Synthesis of tetranuclear complexes $py_3Cu_3MCl_4O_2$ (M = Co (IVa), Ni (IVb) and Zn (IVd))

The title tetranuclear complexes were obtained by flushing the respective filtrates from the previous section with O_2 for 20 min at room temperature. Manometric O_2 uptake measurements with a standard Warburg apparatus at 25 °C [8] indicated the stoichiometry $\Delta[O_2]/\Delta[\mathbf{II, III}] = 1.00 \pm 0.05$ in eqns. (5)–(7). Cryoscopic measurements on the product solutions indicated the presence of equimolar py, **IV** and the stoichiometric amount of disulfide N_2S_2 in eqns. (5) and (6). Cryoscopic measurements on the solution obtained by oxidation of **IIc** indicated the formation of **Ib** and the stoichiometric amount of N_2S_2. Attempted isolation of solid products **Ib, IVa, IVb** and **IVd** from solution led to disproportionation to give partially soluble materials that are very weak initiators for reaction (1) (R = Me) [12, 15, 17, 24].

Synthesis of 3,3', 5,5'-tetramethyl-1,4-diphenoquinone (DPQ)

The product of reaction (1b) (R = Me) was obtained by adding, in one portion, 3.0 ml of a solution of **Ib** [12, 15] (1.0 mM in nitrobenzene) to a large excess of DMPOH in nitrobenzene (10 ml). The solution was vigorously flushed with a stream of O_2 for 2 h at room temperature, then poured into methanol (150 ml) containing HCl (12 M, 2 ml). The DPQ product that immediately precipitated was washed with methanol and recrystallized from methylene chloride/diethyl ether.

Physical measurements

The electronic spectra of **Ib, II** and **III** and of the product solutions from reactions (5)–(8) in nitrobenzene were measured under N_2 with Perkin–Elmer Lambda 4B and Beckman DK-1A spectrophotometers in matched quartz cells at room temperature. The rates of reactions (5)–(8) in nitrobenzene were measured by monitoring absorbance increases as a function of time at fixed wavelength in the region 750–850 nm in the Lambda 4B instrument with **II** or **III** in pseudo-first-order excess. The total reactant concentration range was $[\mathbf{II, III}]_0 = 4.0$–$14.0$ mM, with $[O_2]_0 = 0.44$ mM. Temperature was controlled to ±0.05 °C in the range 18.0–47.0 °C. Pseudo-first-order rate constants k_{obs} were obtained from the slopes of linear plots of $\ln(A_\infty - A_t)$ versus time, where A_t is the absorbance at fixed wavelength and temperature at time t. Each run was repeated at least three times under fixed experimental conditions to establish an upper limit of ±4% for each reported rate constant.

Similar procedures were used to monitor the oxidation of 2,6-dimethylphenol (DMPOH) by **Ib, IVa, IVb** and **IVd** in nitrobenzene. The reactions were run with DMPOH in pseudo-first-order excess in the range 2.9–124 mM both in the presence and absence of O_2. Temperature was varied in the range 15.0–42.0 °C. The reaction stoichiometries $S = \Delta[\text{DPQ}]/\Delta[\mathbf{Ib, IV}]$ were measured at 431 nm, where DPQ has a pronounced absorption maximum.

Results and discussion

Transmetalation of $[pyCuCl]_4$ with reagents $M(NS)_2$ (A: M = Co, Ni, Cu and Zn) and $Co(NS)_3$ (B)

Pale yellow nitrobenzene solutions of $[pyCuCl]_4$ [15] react with equimolar **A** (M = Co, Ni, Cu or Zn) or **B** at room temperature under N_2 to give 1 mol each of respective tetranuclear products $py_3Cu_3M(NS)Cl_4$ (**IIa–d**) and $py_3Cu_3Co(NS)_2Cl_4$ (**III**), py and insoluble Cu(NS)(s), as indicated by gravimetric determination of Cu(NS)(s) [18–20] and cryoscopic measurements [8] of the product filtrates (eqns. (3) and (4) and Table 1). The reactions were all complete in 6 h at room temperature under typical [18] reaction conditions. These results are exactly analogous to the systems with *N,N*-diethylnicotinamide (N) as the copper(I) target ligand [18–20].

Electronic spectra of IIa–d and III

Nitrobenzene solutions of pale yellow copper(I)-containing complexes $[pyCuCl]_4$, **IIb** (M = Ni) and **IId** (M = Zn), have very low absorptivity and no spectral features in the region 500–900 nm (Table 1). However, copper–cobalt complexes **IIa** and **III** are blue and green, respectively, because of spectral maxima centered at 610 nm (Fig. 1). These structured features are characteristic of five-coordinate cobalt(II) [18–20, 27]. Figure 1 demonstrates an increase of cobalt(II) absorptivity on increasing the number of coordinated NS ligands. The maximum molar absorptivities of **IIa** and **III** are 680 and 970 M^{-1} cm^{-1}, respectively, in nitrobenzene at 25 °C; those of the analogous complexes $N_3Cu_3Co(NS)Cl_4$ and $N_3Cu_3Co(NS)_2Cl_4$ (N = *N,N*-diethylnicotinamide) are 830 [18] and 890 [19] M^{-1} cm^{-1}, respectively. The stoichiometric ratio (py, N)/Cu = 1.0 for all these complexes strongly suggests that py and N are only coordinated by their copper centers.

The observed cobalt absorptivity differences could be due to small geometric differences at cobalt in essentially the same 'cubane' [18–20] core structure or differences in the extent of intramolecular copper–cobalt electronic coupling (see below) [18–20, 28].

Comparison of the three spectra in Fig. 1 shows that **III** contains a Cl_3Cu^{II} center that characteristically absorbs in the 700–900 nm region [29]. The molar absorptivities ϵ_{850} of $[NCuCl]_4O_2$ [8], $[pyCuCl]_4O_2$ (**Ib**) [12, 15] and **III** are 770, 810 and 185 M^{-1} cm^{-1},

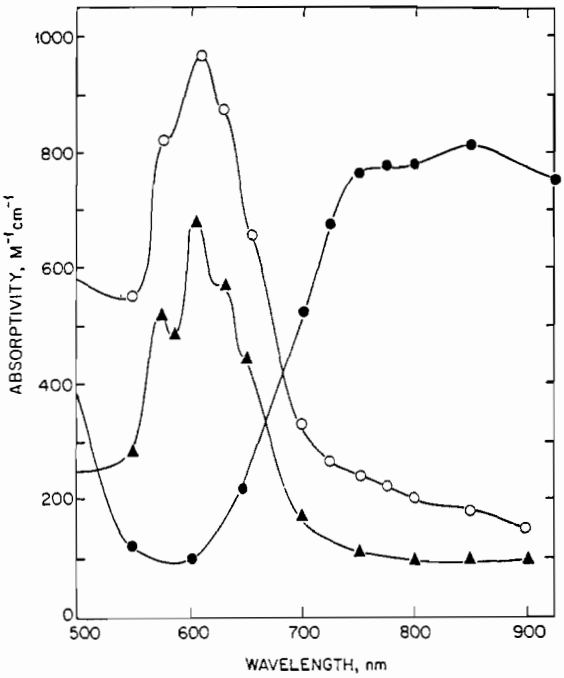

Fig. 1. Electronic spectra of $[pyCuCl]_4O_2$ (**Ib**, ●), $py_3Cu_3Co(NS)_2Cl_4$ (**III**, ○) and $py_3Cu_3Co(NS)Cl_4$ (**IIa**, ▲) in nitrobenzene at 25 °C.

respectively, in nitrobenzene at 25 °C. Neglecting minor copper(I) absorption in **III** (see above), the respective atomic copper(II) absorptivities (190, 203 and 185 (g atom $Cu^{II})^{-1}$ cm^{-1}) are lowest for **III**, which has the largest ϵ_{610} and no distinct absorption minimum at 700 nm like that seen for $N_3Cu_3Co(NS)_2Cl_4$ [19]. Cryoscopic measurements (Table 1) indicate that the unusual ϵ_{610} and ϵ_{850} for **III** are not due to coordination of py by cobalt(II). They are ascribed to geometrical differences at the copper(II) and cobalt(II) centers of $N_3Cu_3Co(NS)_2Cl_4$ and **III** in essentially the same 'cubane' core structure and/or different extents of electron transfer within the formalism [19, 28] $Cu^I_3Co^{II}(NS)_2Cl_4 \leftrightarrow Cu^I_2Cu^{II}Co^{III}(NS)_2Cl_4$.

Stoichiometry and products of oxidation of $[pyCuCl]_4$, IIa–d and III by O_2 in nitrobenzene

Manometric O_2 measurements showed that the title reactions obey the stoichiometry of eqns. (5)–(7). Only the copper(I) centers and coordinated NS ligands of **II** and **III** are oxidized by O_2, exactly as found with ligands N [18–20]. Attempted isolation of the oxidized metal-containing products by gel permeation chromatography and selective precipitation gave weakly catalytic solid products with very variable solubility in nitrobenzene. However, cryoscopic measurements on the product solutions were consistent with their formulation as shown in eqns. (5)–(7). The disulfide coproduct N_2S_2 of eqns. (5)–(7) was isolated by chromatography and identified by comparison with an authentic sample [18]. The product solution from oxidation of **IIc** was identified by comparison of its spectrum with that of a mixture of authentic **Ib** [12, 15] and N_2S_2 in nitrobenzene at the stoichiometric ratio of eqn. (7) (see below).

Electronic spectra of Ib and IVa, IVb and IVd

The electronic spectra of the oxidized product solutions from reactions (5)–(7) are shown in Fig. 2. Comparison with Fig. 1 shows the increase in absorptivity due to oxidation of copper(I) in **II** and **III** to copper(II) in **Ib** and the respective **IV**.

A variety of evidence suggests that the products of eqns. (5)–(7) with N replacing py and M = Co, Ni, Cu and Zn have core structure **V** [18–20, 27, 28]. The characteristic properties of **V** are that: (i) they can easily be obtained as re-dissolvable solids (although they disproportionate on attempted crystallization); (ii) their electronic spectra are insensitive to the presence of oxidation co-product N_2S_2; (iii) $\epsilon_{850} \simeq 700$ M^{-1} cm^{-1} is essentially independent of M [18–20]; (iv) the spectra exhibit pronounced absorption minima near 600 nm;

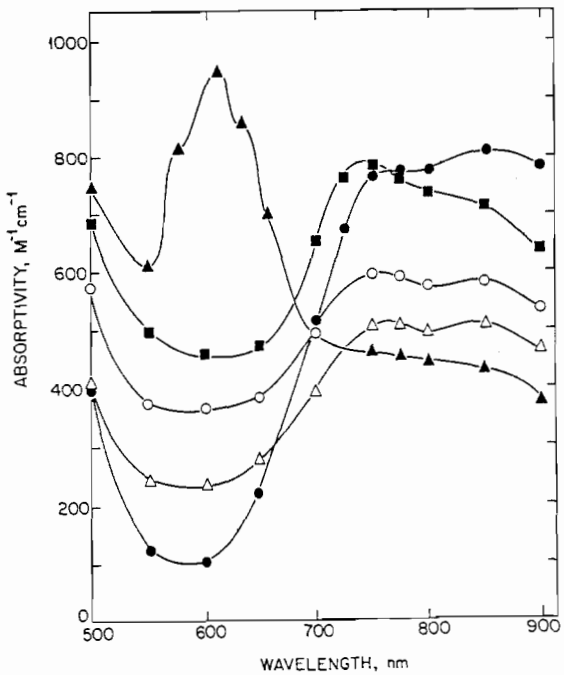

Fig. 2. Electronic spectra of $[pyCuCl]_4O_2$ (**Ib**, ●), **Ib** in the solution from reaction (7) (■), $py_3Cu_3CoCl_4O_2$ (**IVa**) in the solution from reaction (5) (M = Co) or (6) (▲), $py_3Cu_3NiCl_4O_2$ in the solution from reaction (5) (M = Ni, O) and $py_3Cu_3ZnCl_4O_2$ in the solution from reaction (5) (M = Zn, Δ). The solvent is nitrobenzene at 25 °C and the concentration of py is 1.0 mM for the solutions generated from reactions (5) and (6). The concentration of N_2S_2 is 0.5 mM for solutions generated in eqn. (5) and 1.0 mM for the solutions generated in eqns. (6) and (7).

and (v) **V** are, at best, very weak initiators for reactions (1) [12, 18–20, 27, 28].

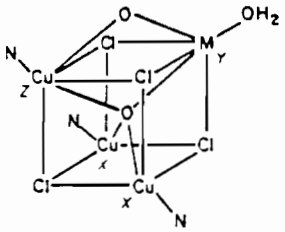

V

The metallic products of eqns. (5)–(7) cannot be obtained as soluble, catalytically-active solids despite the fact that the product solutions from eqns. (5)–(7) are active in reaction (1b) (see below). The second major difference between $N_3Cu_3MCl_4O_2$ products and those from eqns. (5)–(7) is that the latter have electronic spectra with only shallow absorption minima (Fig. 2). Since the spectra of $py_3Cu_4Cl_4O_2$ (**Ia**) and $[pyCuCl]_4O_2$ (**Ib**) are similar and have deep minima near 600 nm [12, 15], it is possible that the spectra in Fig. 2 are affected by the presence of oxidation co-product N_2S_2 from reactions (5)–(7).

This possibility was checked by deliberate addition of small amounts of N_2S_2 [18] to the product solutions from eqns. (5)–(7) and re-examination of their spectra. We found that addition of 0.5 mol N_2S_2 to solutions of **Ib** from eqns. (7) or (8) [15] and **IVd** (from eqn. (5) (M=Zn)) altered their spectra by

$$[pyCuCl]_4 + O_2 \longrightarrow \mathbf{Ib} \qquad (8)$$

increasing the minimum absorbance at *c.* 600 nm (Fig. 3), while the spectra of solutions of **IVa** (from eqns. (5) (M=Co) and (6)) and **IVb** (from eqn. (5) (M=Ni)) were unaffected. As pointed out earlier, comparison

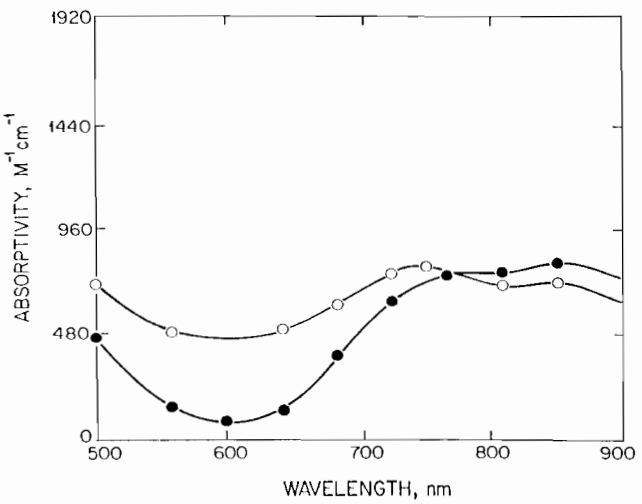

Fig. 3. Electronic spectra of $[pyCuCl]_4O_2$ (**Ib**, ●) and of a solution containing **Ib** and N_2S_2 (○) (both 1.0 mM) in nitrobenzene at 25 °C.

of Figs. 2 and 3 indicates that the products of oxidation of equimolar $py_3Cu_3Cu(NS)Cl_4$ (**IIc**) and py from eqn. (3) by O_2 are **Ib** and N_2S_2 (Fig. 3).

The spectral changes on addition of N_2S_2 evidently are due to coordination of N_2S_2 to particular copper(II) centers of **Ib** and **IVd**. The coordination of N_2S_2 must be weak because: (i) N_2S_2 is a poor ligand [18]: (ii) we can interpret the cryoscopic properties of the product solutions from eqns. (5)–(7) without having to account for coordination of N_2S_2; and (iii) the addition of modest amounts of N_2S_2 to solutions of **Ib** and **IV** has no effect on their rates of oxidation of DMPOH (see below).

We propose that $py_3Cu_3(Co, Ni)Cl_4O_2$ (**IVa** and **IVb**) and $py_3Cu_3ZnCl_4O_2$ (**IVd**) have the different core structures shown in Scheme 2. Core structures **V** [18–20] and **IVa, b** do not significantly interact with N_2S_2 or initiate reaction (1), while weak coordination of N_2S_2 to the Cu_v sites of **Ia, Ib** and **IVd** alters their spectra.

This proposal is supported by the following observations. (i) The Cu_x sites in **Ib** and **IVd** approximate those in $(\mu_4\text{-O})py_4Cu_4Cl_6$, (**VI**) [30], but the spectrum of **VI** in nitrobenzene is unaffected by addition of equimolar N_2S_2. This supports weak N_2S_2 interaction with the Cu_v site of **Ib** and **IVd**; (ii) py at Cu_v is selectively replaced by *N,N,N'N'*-tetraethylethylenediamine [12]; and (iii) the characteristics of **Ia, Ib** and **IVd** differ from those of **IVa** and **IVb** in their reactions with DMPOH (see below).

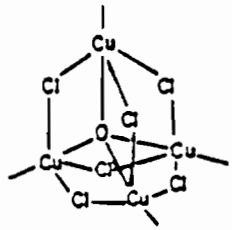

VI

On this basis, the spectra of **IVa** and **IVb** in Fig. 2 are those of the actual molecules, while those for the product solutions from reactions (5) (M=Zn) and (7) are not those of **Ib** and **IVd**, respectively, because of the presence of co-product N_2S_2. Nevertheless, the 700–900 nm molar absorptivities of **IVa, IVb** and **IVd** are about 75% of that of **Ib** (Fig. 2) because they contain three copper(II) centers and their M centers do not absorb appreciably in this region [12, 18–20].

Kinetics of oxidation of II *and* III *by* O_2 *in nitrobenzene*

In this section we present data for the oxidation of excess copper complexes $[pyCuCl]_4$, **II** and **III** by O_2 (eqns. (5)–(8) [15]) in nitrobenzene. The reactions were easily monitored by spectrophotometry in the wavelength region 700–900 nm, where large absorbance increases are observed. Wide temperature ranges were

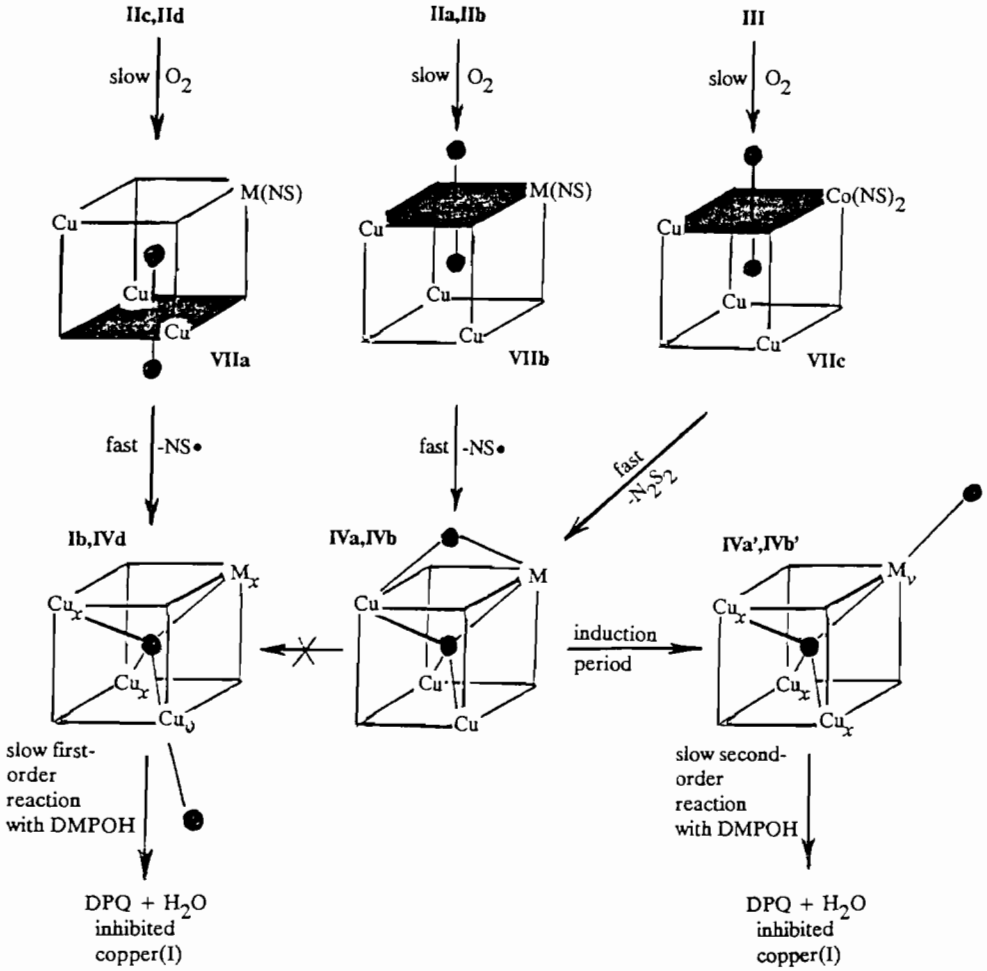

Scheme 2.

employed to allow the estimation of precise activation parameters. Each copper reactant was present in sufficient excess to ensure pseudo-first-order conditions.

Plots of $\ln(A_\infty - A_t)$ versus time, where A_t is the absorbance at time t, were linear for at least four half-lives in each system (Fig. 4), with no evidence for reaction precursors or intermediates. This indicates a rate law that is first order in $[O_2]$ and that the oxidation of coordinated NS in **II** and **III** is much faster than the rate-determining step [18–20]. The derived first-order rate constants k_{obs} were accurately proportional to **[II]** or **[III]** at fixed temperature and passed through the origin (Fig. 5). This establishes that reactions (5)–(8) are irreversible and have simple rate law (9), where k_T is the second-order rate constant. The kinetic data are collected in Table 2.

$$\text{rate} = k_T[[\text{pyCuCl}]_4, \textbf{II}, \textbf{III}][O_2] \quad (9)$$

Interpretation of the kinetic data

A variety of evidence indicates that the rate-determining step of oxidation of tetranuclear halo(pyridine)-copper(I) complexes is insertion of the O_2 molecule through their X_4 core of halogen atoms [8, 15, 18, 19]. Most of the activation parameters in Table 2 fit the correlation in Fig. 6 and strongly support an insertion mechanism for reactions (5)–(8).

The deviant points are for oxidation of $[\text{pyCuCl}]_4$ [15] and $[\text{py}_2\text{CuCl}]_4$ [8], which contain more py ligands than the other reactants. This leads to the largest k_T and the lowest activation enthalpies $\Delta H_T^{\ddagger}$, consistent with 'loosening' of the reductant core by coordinated py [8, 15]; $\Delta H_T^{\ddagger}$ is unusually large for oxidation of $(\text{py, N})_3\text{Cu}_3\text{ZnCl}_4$ complexes, a property attributed to the isoelectronic configuration of copper(I) and zinc(II) (both d^{10}) but a higher nuclear charge for Zn which 'stiffens' the molecular core [18]. All the reactions have very negative $\Delta S_T^{\ddagger}$, which is the hallmark of an associative oxidation mechanism.

The second-order rate constant k_T for oxidation of **IIa** is about twice that for oxidation of **III** at 25 °C in nitrobenzene (Table 2). The corresponding ratio for the pair $N_3Cu_3Co(NS)Cl_4$ and $N_3Cu_3Co(NS)_2Cl_4$ is about ten. Two likely factors responsible for these

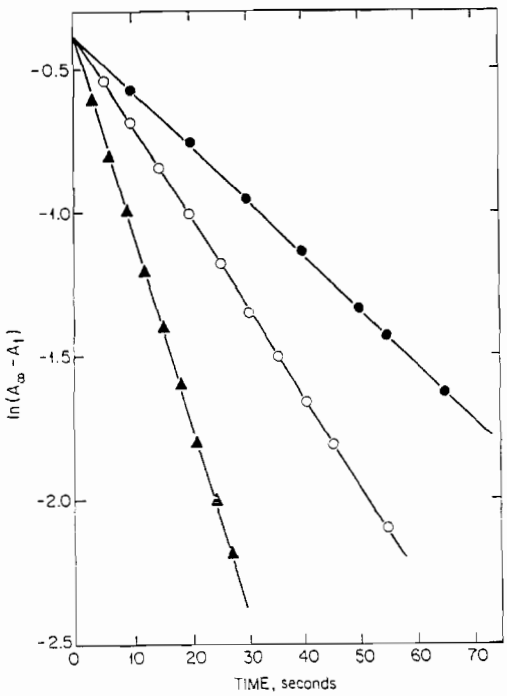

Fig. 4. First-order kinetic plot for the reaction of $py_3Cu_3Zn(NS)Cl_4$ (**IId**) with O_2 (0.44 mM) in nitrobenzene at 25 °C. The concentrations (mM) of **IVd** are 4.0 (●), 6.0 (○) and 9.0 (▲).

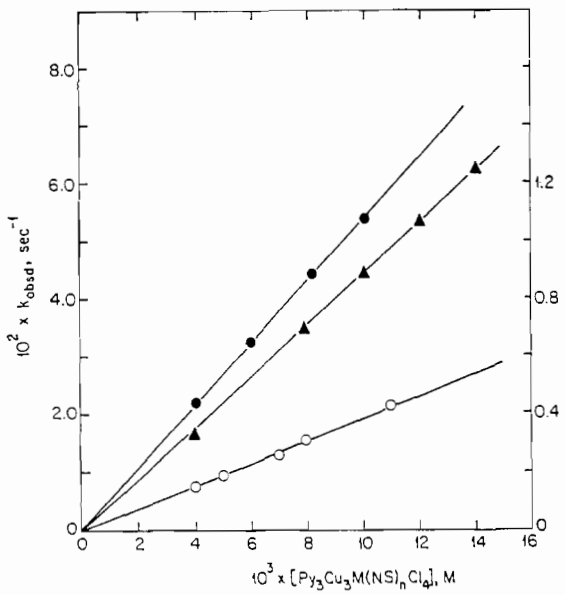

Fig. 5. Plots of the first-order rate constants k_{obs} *vs.* [reductant] for oxidation of the following complexes by O_2 in nitrobenzene at 25 °C: $[pyCuCl]_4$ (left ordinate, ●), $py_3Cu_3Co(NS)Cl_4$ (**IIa**, right ordinate, ▲) and $py_3Cu_3Co(NS)Cl_4$ (**III**, right ordinate, ○).

TABLE 2. Kinetic parameters for oxidation of $[py_2CuCl]_4$, $[(py, N)CuCl]_4$, $(py, N)_3Cu_3M(NS)Cl_4$ and $(py, N)_3Cu_3Co(NS)_2Cl_4$ complexes by dioxygen in nitrobenzene

Symbol	Reactant	k_T[a]	$\Delta H_T^{\ddagger}$[b]	$\Delta S_T^{\ddagger}$[c]
	$[py_2CuCl]_4$[d]	770	2.9	−36
	$[pyCuCl]_4$[e]	110	2.1	−58
IIa	$py_3Cu_3Co(NS)Cl_4$	4.1	3.6	−44
III	$py_3Cu_3Co(NS)_2Cl_4$	1.8	9.6	−26
IIb	$py_3Cu_3Ni(NS)Cl_4$	15	4.5	−38
IIc	$py_3Cu_3Cu(NS)Cl_4$	4.6	6.1	−35
IId	$py_3Cu_3Zn(NS)Cl_4$	5.6	8.7	−26
	$[NCuCl]_4$[f]	16	3.9	−40
	$N_3Cu_3Co(NS)Cl_4$[g]	5.4	4.3	−41
	$N_3Cu_3Co(NS)_2Cl_4$[h]	0.53	3.1	−49
	$N_3Cu_3Ni(NS)Cl_4$[g]	5.1	4.7	−40
	$N_3Cu_3Zn(NS)Cl_4$[g]	3.7	8.4	−26

[a]Units are M^{-1} set^{-1} at 25 °C. [b]Units are kcal mol^{-1}; typical error is ±0.3 kcal mol^{-1}. [c]Units are cal deg^{-1} mol^{-1} at 25 °C; typical error is ±3 cal deg^{-1} mol^{-1}. [d]Data from ref. 8. [e]Data from ref. 15. [f]Data from ref. 31. [g]Data from ref. 18. [h]Data from ref. 19.

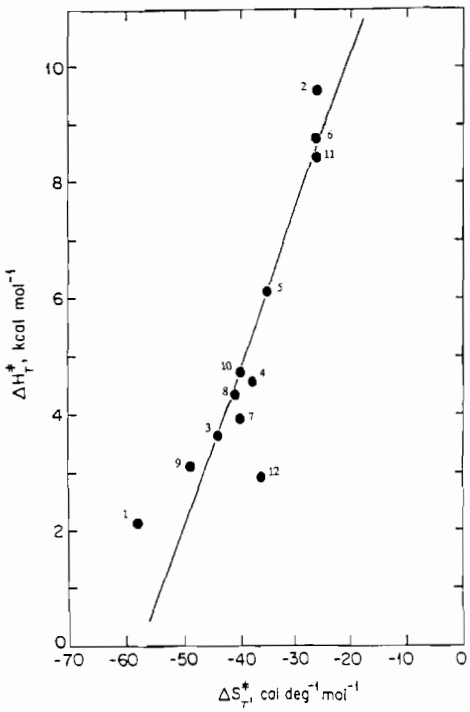

Fig. 6. Plot of $\Delta H_T^{\ddagger}$ *vs.* $\Delta S_T^{\ddagger}$ at 25 °C for oxidation of the following complexes by O_2 in nitrobenzene: 1, $[pyCuCl]_4$; 2, $py_3Cu_3Co(NS)_2Cl_4$ (**III**); 3, $py_3Cu_3Co(NS)Cl_4$ (**IIa**); 4, $py_3Cu_3Ni(NS)Cl_4$; 5, $py_3Cu_3Cu(NS)Cl_4$ (**IIc**); 6, $py_3Cu_3Zn(NS)Cl_4$ (**IId**); 7, $[NCuCl]_4$ [31]; 8, $N_3Cu_3Co(NS)_2Cl_4$ [19]; 9, $N_3Cu_3Co(NS)Cl_4$ [18]; 10, $N_3Cu_3Ni(NS)Cl_4$ [18]; 11, $N_3Cu_3Zn(NS)Cl_4$ [18]; 12, $[py_2CuCl]_4$ [8].

differences are that: (i) insertion of O_2 through particular faces is obstructed by the two large NS ligands on the cobalt(II) center of **III**; and (ii) the presence of one formal copper(II) center in **III** stiffens the molecular core relative to those in $[pyCuCl]_4$ and **II**, which contain no copper(II).

As a group, $(N, py)_3Cu_3M(NS)Cl_4$ complexes react with O_2 in nitrobenzene with k_T from 3.7 to 5.6 M^{-1}

s^{-1} at 25 °C with the exception of **IIb** ($k_T = 15$ M^{-1} s^{-1}), which might have a slightly different core structure. All these rates are much lower than for oxidation of $[pyCuCl]_4$ and $[py_2CuCl]_4$, which indicates that obstruction of O_2 insertion by coordinated NS is a real effect.

In general, the substitution of one $M(NS)_{1,2}$ center for one (py, N)Cu center in $[(py, N)CuX]_4$ complexes seems to have two effects: (i) the X_4 core stiffens because of the higher nuclear charge on M (this is particularly noticeable with M = Zn, see above); (ii) O_2 insertion through three of the six faces of (py, $N)Cu_3M(NS)_{1,2}X_4$ seems to be obstructed by the NS ligand system.

Stoichiometry of oxidation of 2,6-dimethylphenol by tetranuclear dioxocopper(II) complexes in nitrobenzene

The product DPQ of reaction (1b) dissolves in nitrobenzene to give red solutions, with a sharp absorption maximum at 431 nm (ϵ 5.1×10^4 M^{-1} cm^{-1} [15]). Equation (10) represents the stoichiometric oxidation of 2,6-dimethylphenol (DMPOH) by **Ib** in nitrobenzene. If reaction (8) is inhibited, say by water from eqn. (10), then stoichiometry $S = \Delta[DPQ]/\Delta[\mathbf{Ib}] = 1.0$, whereas if it is not then the system is catalytic [15].

$$\mathbf{Ib} + 2DMPOH \longrightarrow [pyCuCl]_4 + DPQ + 2H_2O \qquad (10)$$

DMPOH was added to a 9.45×10^{-5} M solution of **Ib** or **IV** in nitrobenzene under O_2 at 25 °C so that [DMPOH] = 8.5 mM. Reaction (1b) was monitored to completion and S was calculated from absorption measurements at 431 nm. We found that S was 0.91–1.06 (Table 3) and was independent of [DMPOH] in the range 2.9–94 mM and reaction temperature. Most importantly, (i) plots of ln $(A_\infty - A_t)$ versus time were linear to at least four half-lives at 431 nm (Fig. 7), indicating a first-order dependence on [oxidant]; (ii) $S \not> 1.0$ even if O_2 was continuously bubbled through the solution; and (iii) S was independent of the presence of O_2.

Linear first-order plots indicate that inhibition of catalysis in reaction (1b) is not due to changes in the oxidant species during their reduction by DMPOH because this would result in non-linear plots reflecting the formation of more or less reactive copper(II) oxidants. $S \simeq 1.0$ is due to inhibition of reoxidation of copper(I) species by O_2 by water from reactions (1b) or (10) [15], as confirmed by separate experiments which showed that rigorously dry conditions are necessary to obtain reproducible kinetic data for reactions (5)–(8). We also found that [DMPOH] > 100 mM is necessary for $S > 1.0$, confirming that inhibition of copper(I) reoxidation reactions by co-product water is less pronounced at high phenol concentrations [15]. It is also evident that O_2 is not involved in the production of DPQ at modest [DMPOH].

We added the product solutions from the reactions of **Ib** and **IV** with DMPOH to methanol containing HCl in an attempt to precipitate polyphenylene oxide from reaction (1a), but none was found. It thus appears that water very effectively inhibits copper(I) reoxidation in these systems. Fortunately, inhibition of catalysis by water isolates the initiation step of oxidation of DMPOH by the copper(II) complexes of this study and enables us to see the real benefits of a transmetalation approach to determining the slowest catalytic component.

Kinetics of oxidation of 2,6-dimethylphenol by tetranuclear dioxo(pyridine)copper(II) complexes in nitrobenzene

The kinetics of oxidation of DMPOH by **Ib, IVa, IVb** and **IVd** were measured in nitrobenzene over the temperature range 15.0–42.0 °C with [DMPOH] = 2.9 − 124 mM in pseudo-first-order excess. DPQ formation was monitored at 431 nm by conventional spectrophotometry in each system.

We found that DPQ formation is first-order under these circumstances (Fig. 7), that the systems obey

TABLE 3. Kinetic parameters and stoichiometry data for oxidation of 2,6-dimethylphenol by $py_3Cu_4Cl_4O_2$, $[pyCuCl]_4O_2$ and $py_3CuMCl_4O_2$ complexes (M = Co, Ni, Zn) in nitrobenzene

Symbol	Complex	10^4 k_{obs}[a]	$k_{11,12}$	$\Delta H^{\ddagger b}_{11,12}$	$\Delta S^{\ddagger c}_{11,12}$	S[d]
Ia[e]	$py_3Cu_3Cl_4O_2$	9.8	9.8×10^{-4}[f]	20.2	−7	1.06
Ib[e]	$[PyCuCl]_4O_2$	9.6	9.6×10^{-4}[f]	20.2	−7	1.03
Ib[g]	$[pyCuCl]_4O_2$	9.6	9.6×10^{-4}[f]	20.1	−7	1.03
IVd[h]	$py_3Cu_3ZnCl_4O_2$	8.0	8.0×10^{-4}[f]	18.4	−10	1.00
IVa[i]	$py_3Cu_3CoCl_4O_2$	2.8[j]	3.3×10^{-2}[k]	10.1	−22	0.91
IVb[l]	$py_3Cu_3NiCl_4O_2$	3.7[j]	4.3×10^{-2}[k]	15.5	−12	0.96

[a]Observed rate constant for DPQ formation with [DMPOH] = 8.5 mM at 21 °C. Units are s^{-1}. [b]Units are kcal mol^{-1}; typical error is ±0.3 kcal mol^{-1}. [c]Units are cal deg^{-1} mol^{-1} at 25 °C; typical error is ±2 cal deg^{-1} mol^{-1}. [d]$S = \Delta[DPQ]/\Delta[oxidant]$ at 21 °C. [e]Data from ref. 15. [f]Units are s^{-1} at 21 °C. [g]Oxidant generated in reaction (7). [h]Oxidant generated in reaction (5) (M = Zn) [i]Oxidant generated in reaction (5) (M = Co) or (6). [j]Induction period observed. See text. [k]Units are M^{-1} s^{-1} at 21 °C. [l]Oxidant generated in reaction (5) (M = Ni).

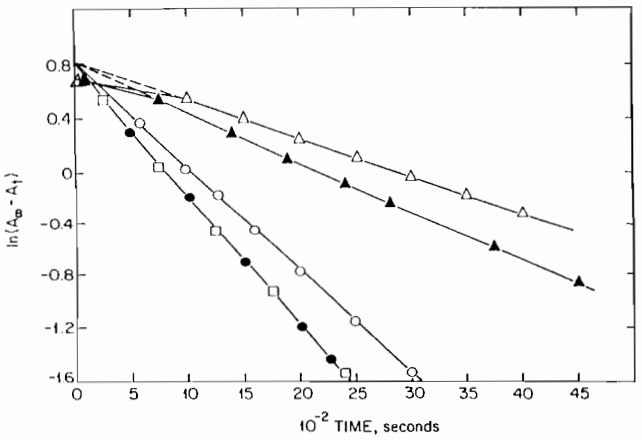

Fig. 7. First-order kinetic plots for the oxidation of excess 2,6-dimethylphenol (DMPOH) to the diphenoquinone (DPQ) in nitrobenzene at 21.0 °C by the following complexes: $[pyCuCl]_4O_2$ (**Ib**, ●), $py_3Cu_4Cl_4O_2$ (**Ia**, □), $py_3Cu_3ZnCl_4O_2$ (**IVd**, ○), $py_3Cu_3CoCl_4O_2$ (**IVa**, △) and $py_3Cu_3NiCl_4O_2$ (**IVb**, ▲). Note the induction period in the last two systems. $[DMPOH]_0 = 8.5$ mM throughout.

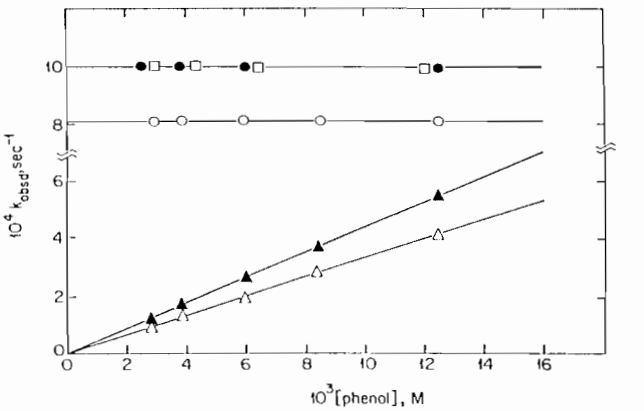

Fig. 8. Plots of k_{obs} *vs.* [DMPOH] for the oxidation of DMPOH in nitrobenzene at 21.0 °C by the following complexes: $[pyCuCl]_4O_2$ (**Ib**, ●), $py_3Cu_4Cl_4O_2$ (**Ia**, □), $py_3Cu_3ZnCl_4O_2$ (**IVd**, ○), $py_3Cu_3CoCl_4O_2$ (**IVa**, △) and $py_3Cu_3NiCl_4O_2$ (**IVb**, ▲). Note that the first three systems are first order, while the last two systems are second order.

second-order rate law (11) or first-order rate law (12), depending on the oxidant (Fig. 8), and that the second-order systems have induction periods (Fig. 7). The symbols **IVa'** and **IVb'** in eqn. (11) are explained below. The kinetic data are collected in Table 3.

$$d[DPQ]/dt = k_{11}[\mathbf{IVa'}, \mathbf{IVb'}][DMPOH] \quad (11)$$

$$d[DPQ]/dt = k_{12}[\mathbf{Ia}, \mathbf{IVd}] \quad (12)$$

We proposed earlier from spectral measurements that $py_3Cu_3ZnCl_4O_2$ (**IVd**) has a core structure that contains a terminal oxo group, while $py_3Cu_3CoCl_4O_2$ (**IVa**) and $py_3Cu_3NiCl_4O_2$ (**IVb**) have a core structure that does not (Scheme 2). The kinetic observations (Figs. 7 and 8, Table 3) support this idea: **Ib** and **IVd** reactions with DMPOH have no induction period (Fig. 7) and oxidize DMPOH with first-order rate law (12), while **IVa** and **IVb** exhibit induction periods and then oxidize DMPOH with second-order rate law (11).

The induction periods were independent of increasing [DMPOH] at room temperature, evidently because **IVa** and **IVb** are weak protic bases [18–20].

Interpretation

We propose the following mechanism to establish a relationship between observed rate laws (11) and (12). Since rate law (11) is second order, we restrict our model to monophenolate complexes in rapid equilibrium (13). With DMPOH in large excess and reaction (14) rate-determining, the pseudo-first-order rate constant k_{obs} is given by eqn. (15).

$$\text{oxidant} + \text{DMPOH} \rightleftharpoons \text{complex} \qquad K_{13} \quad (13)$$

$$\text{complex} \longrightarrow \text{products} \qquad k_{14} \quad (14)$$

$$d[DPQ]/dt = K_{13}k_{14}[\text{oxidant}][DMPOH]/(1 + K_{13}[DMPOH]) \quad (15)$$

This rate law is not obeyed by any of the systems investigated (Fig. 8). The two limits of eqn. (15) are $K_{13}[DMPOH] \ll 1$ and $K_{13}[DMPOH] \gg 1$. The first leads to eqn. (16), which has the same form as eqn. (11), with $k_{11} = K_{13}k_{14}$. The second leads to eqn. (17), which corresponds to first-order rate law (12) with $k_{12} = k_{14}$. The observation of rate law (12) strongly suggests that it is the special case with very strong phenol coordination by oxidants **Ia** and **IVd**. All the reactions have negative $\Delta S^{\ddagger}$ which indicate an associative mechanism.

$$d[DPQ]/dt = K_{13}k_{14}[\text{oxidant}][DMPOH] \quad (16)$$

$$d[DPQ]/dt = k_{14}[\text{oxidant}] \quad (17)$$

Previous evidence that **Ia** and **Ib** oxidize DMPOH at identical rates with first-order rate law (12) has been explained by formation of strong complex $(\mu_4\text{-}O)py_3Cu_4Cl_4(ODMP)_2$ with formation constant 7×10^7 M^{-2} at 32 °C in nitrobenzene [15]. DMPOH evidently is a good substrate for structure **IVd** because it is deprotonated by the terminal oxo group (Scheme 2). The same first-order rate law (12) with **Ia, Ib** [15] or **IVd** as oxidants of DMPOH suggests that they all contain a strongly basic Cu_v–O site and that Zn is at an *x* site. This explains why **IVd** oxidizes DMPOH at about 75% of the rate of its oxidation by **Ia**, which has four copper(II) centers (Fig. 8 and Table 3).

Cryoscopic evidence indicates that the M centers in complexes **IVa, IVb** and **IVd** do not coordinate py. Now we ask if M in these complexes is at site *v*, site *x* or neither.

Second-order rate law (11) for oxidation of DMPOH by **IVa'** and **IVb'** (Scheme 2) corresponds to $K_{13} < 10^{-5}$ M^{-1} in these systems. The observed induction period is not affected by moderate amounts of DMPOH, confirming that **IVa** and **IVb** also are very weak bases. This is consistent with a core structure that contains a μ-oxo group that is too weakly basic to deprotonate DMPOH (Scheme 2) [8, 18, 19].

The induction period is the time taken for structure **IVa** or **IVb** to respond to the presence of DMPOH. Its μ-oxo group could open to leave a Cu_v–O site in the analogue of **IVd** or a M_v–O site in **IVa'** and **IVb'** (Scheme 2). The second event is favored because M_v–O (M = Co (d^7) or Ni (d^8) should be much less basic than Cu_v–O (d^9), all of whose d-orbitals contain electrons [16]. We thus propose that, after the induction period, DMPOH is oxidized by **IVa'** and **IVb'** that contain weakly basic M_v–O sites. An induction period that resulted in homologues of structure **IVd** would create a Cu_v–O site and result in rate law (12), which is not observed for the reactions of **IVa** and **IVb** with DMPOH.

Origin of different core structures

We offer the explanation in Scheme 2 for the formation of different core structures **IVa, b** and **Ib, IVd** in reactions (5)–(8). Ligands py and Cl have been omitted and the O atoms of O_2 are shown as filled circles to clarify discussion. Transition states **VIIa–c** represent different extents of O_2 insertion through reductants **IIc** and **IId, IIa** and **IIb**, and **III**, respectively. Molecule O_2 has entered from the lower face (the left and front faces of the cubanes are equivalent) to avoid the obstructing NS ligands (Table 2).

The leading atom of O_2 has only reached the center of the cube in **VIIa**. Transfer of the third electron to O_2 at this point in time breaks its O–O bond, leaving the leading O atom as a μ_4-O group at the center. Transfer of the fourth electron creates a Cu_v–O site in product structures **Ib** and **IVd**.

The O_2 molecule has traversed further through the reductant core in transition states **VIIb** and **VIIc** (the extent has been emphasized in Scheme 2 to make the distinction). Transfer of the third electron to O_2 at this point in time breaks the O–O bond and leaves the trailing O atom as a central μ_4-O group. The leading O atom becomes a μ-O group that is bonded to M because M mediates transfer of the fourth electron to O from coordinated NS^- in **IIa** and **IIb**. It is conceivable that this gives structure **IVa'** in the oxidation of **III**: reductant **III** contains only two copper(I) centers, so the third and fourth electrons must come from its two coordinated NS^- ligands. However, the products of oxidation of **IIa** and **III** are identical in all respects. The third or fourth electron must come from copper(I) in **IIa** and **IIb**, which naturally leaves the oxide product bonded as a μ-O to copper(II). Creation of structures **IVa'** and **IVb'** in the oxidations of **IIa, IIb** and **III** would leave no explanation of the induction periods in the reactions of **IVa** and **IVb** with DMPOH. We prefer to think that **IVa'** and **IVb'** are created in the induction period (Scheme 2).

To summarize, it appears that different product core structures in reactions (5)–(8) occur because the third electron is transferred to O_2 at different points in its traversal of the respective reductant core structures.

Conclusions

Replacement of one copper(I) center in catalytic complex $[pyCuCl]_4$ with M from $M(NS)_n$ reagents (M = Co, Ni or Zn) gives $pyCu_3M(NS)_{n-1}Cl_4$ species that are oxidized by O_2 to tetranuclear oxocopper(II) products with different molecular core structures. These structures have different affinities for 2,6-dimethylphenol that are reflected by different rate laws for its oxidation to DPQ. It remains to be seen whether $[pyCuCl]_4$ can be progressively transmetalated and then oxidized to give oxidants containing fewer copper(II) centers. This is a worthwhile goal because reduction of the number of copper(II) centers in an oxidant molecule should favor reaction (1a) over (1b). We will report our findings in subsequent papers.

Acknowledgements

We gratefully acknowledge the National Science Foundation (Grants CHE-8717556 and INT-8918985) for financial support of our work. Noralie Barnett and Xiaochun Liu are thanked for skilled technical assistance.

References

1 A. S. Hay, H. S. Blanchard, C. F. Endres and J. W. Eustance, *J. Am. Chem. Soc., 81* (1959) 6335; H. L. Finkbeiner, A. S. Hay and D. M. White, in C. E. Schildnecht and I. Skeist (eds.), *Polymerization Processes*, Wiley–Interscience, New York, 1977, p. 537, and refs. therein.

2 G. Davies and M. A. El-Sayed, in K. D. Karlin and J. A. Zubieta (eds.), *Inorganic and Biochemical Perspectives in Copper Coordination Chemistry*, Adenine, Guilderland, New York, 1983, p. 281, and refs. therein.

3 T. G. Spiro (ed.), *Copper Proteins*, Wiley, New York, 1981.

4 T. R. Demmin, M. D. Swerdloff and M. Rogic, *J. Am. Chem. Soc., 103* (1981) 5795, and refs. therein; K. D. Karlin and Y. Gultneh, *Prog. Inorg. Chem., 35* (1987) 219; Z. Tyeklar and K. D. Karlin, *Acc. Chem. Res., 22* (1989) 241.

5 R. A. Sheldon and J. K. Kochi, *Metal-Catalyzed Oxidation of Organic Compounds*, Academic Press, New York, 1981.

6 A. S. Hay, P. Shenian, A. C. Gowan, P. F. Erhardt, W. R. Haaf and J. E. Therberg, in *Encyclopedia of Polymer Science and Technology,* Interscience, New York, 1969, p. 92.
7 S. Patai (ed.), *The Chemistry of Quinoid Compounds,* Vols. 1 and 2, Wiley, New York, 1975; C. G. Pierpoint and R. M. Buchanan, *Coord. Chem. Rev., 38* (1981) 45.
8 G. Davies and M. A. El-Sayed, *Inorg. Chem., 22* (1983) 1257.
9 G. F. Endres, A. S. Hay and J. W. Eustance, *J. Org. Chem., 28* (1963) 1300.
10 G. W. Parshall, *Homogeneous Catalysis,* Wiley, New York, 1980, p. 133; G. Davies and M. A. El-Sayed, *Comments Inorg. Chem., 4* (1985) 151.
11 G. Davies, M. A. El-Sayed and M. Henary, *Inorg. Chem., 26* (1987) 3266.
12 G. Davies, M. A. El-Sayed, A. El-Toukhy, M. Henary and C. A. Martin, *Inorg. Chem., 25* (1986) 4479.
13 G. Davies, M. A. El-Sayed and R. E. Fasano, *Inorg. Chim. Acta, 71* (1983) 95.
14 I. Bodek and G. Davies, *Inorg. Chem., 17* (1978) 1814.
15 M. A. El-Sayed, A. Abu-Raqabah, G. Davies and A. El-Toukhy, *Inorg. Chem., 28* (1989) 1909.
16 J. M. Mayer, *Comments Inorg. Chem., 8* (1988) 125.
17 A. El-Toukhy, G.-Z. Cai, G. Davies, T. R. Gilbert, K. D. Onan and M. Veidis, *J. Am. Chem. Soc., 106* (1984) 4596.
18 G. Davies, M. A. El-Sayed, A. El-Toukhy, T. R. Gilbert and K. Nabih, *Inorg. Chem., 25* (1986) 1929.
19 G. Davies, M. A. El-Sayed, A. El-Toukhy, M. Henary and T. R. Gilbert, *Inorg. Chem., 25* (1986) 2373.
20 G. Davies, M. A. El-Sayed, A. El-Toukhy, M. Henary, T. S. Kasem and C. A. Martin, *Inorg. Chem., 25* (1986) 3904.
21 G. Davies, M. A. El-Sayed and A. El-Toukhy, *Comments Inorg. Chem., 8* (1989) 203.
22 K. G. Caulton, G. Davies and E. M. Holt, *Polyhedron Rep. 33; Polyhedron, 9* (1990) 2319.
23 G. Davies, M. A. El-Sayed and A. El-Toukhy, *Chem. Soc. Rev.,* in press.
24 G. Davies, M. A. El-Sayed and X. Liu, unpublished results.
25 R. N. Keller and H. D. Wycoff, *Inorg. Synth., 2* (1946) 1.
26 K. D. Onan, G. Davies, M. A. El-Sayed and A. El-Toukhy, *Inorg. Chim. Acta, 119* (1986) 121, and refs. therein.
27 A. Abu-Raqabah, G. Davies, M. A. El-Sayed, A. El-Toukhy and M. Henary, *Inorg. Chem., 28* (1989) 1156.
28 G. Davies, M. A. El-Sayed, A. El-Toukhy and M. Henary, *Inorg. Chim. Acta, 168* (1990) 65.
29 G. Davies, A. El-Toukhy, K. D. Onan and M. Veidis, *Inorg. Chim. Acta, 98* (1985) 85.
30 B. T. Kilbourne and J. D. Dunitz, *Inorg. Chim. Acta 1* (1967) 209.
31 M. R. Churchill, G. Davies, M. A. El-Sayed, J. P. Hutchinson and M. W. Rupich, *Inorg. Chem., 21* (1982) 995.